Remote Sensing of Environment 113 (2009) 1175–1182

Contents lists available at ScienceDirect

Remote Sensing of Environment

journal homepage: www.elsevier.com/locate/rse

A four-band semi-analytical model for estimating chlorophyll a in highly turbid lakes: The case of Taihu Lake, China

Chengfeng Le *, Yunmei Li, Yong Zha, Deyong Sun, Changchun Huang, Heng Lu

Key Laboratory of Virtual Geographic Environment, Ministry of Education, College of Geographic Science, Nanjing Normal University, Nanjing 210046, PR China

ARTICLE INFO

Article history:
Received 18 October 2008
Received in revised form 2 February 2009
Accepted 7 February 2009

Keywords:
Semi-analytical model
Remote sensing
Chlorophyll a
Taihu Lake

ABSTRACT

Accurate estimation of phytoplankton chlorophyll a (Chla) concentration from remotely sensed data is particularly challenging in turbid, productive waters. The objectives of this study are to validate the applicability of a semi-analytical three-band algorithm in estimating Chla concentration in the highly turbid, widely variable waters of Taihu Lake, China, and to improve the algorithm using a proposed four-band algorithm. The improved algorithm is expressed as $[Rrs(\lambda_1)^{-1} - Rrs(\lambda_2)^{-1}][Rrs(\lambda_4)^{-1} - Rrs(\lambda_3)^{-1}]^{-1}$. The two semi-analytical algorithms are calibrated and evaluated against two independent datasets collected from 2007 and 2005 in Taihu Lake. Strong linear relationships were established between measured Chla concentration and that derived from the three-band algorithm of $[Rrs^{-1}(660) - Rrs^{-1}(692)]Rrs(740)$ and the four-band algorithm of $[Rrs^{-1}(662) - Rrs^{-1}(693)][Rrs^{-1}(740) - Rrs^{-1}(705)]^{-1}$. The first algorithm accounts for 87% and 80% variation in Chla concentration in the 2007 and 2005 datasets, respectively. The second algorithm accounts for 97% of variability in Chla concentration for the 2007 dataset and 87% of variation in the 2005 dataset. The three-band algorithm has a mean relative error (MRE) of 43.9% and 34.7% for the 2007 and 2005 datasets. The corresponding figures for the four-band algorithm are 26.7% and 28.4%. This study demonstrates the potential of the four-band model in estimating Chla even in highly turbid case 2 waters.

1. Introduction

It is well acknowledged that water spectral reflectance (Rrs(λ)) in the visible spectrum provides qualitative and quantitative information on optically significant materials present in natural water. The blue and green spectral regions of Rrs(λ) variability are commonly used to assess chlorophyll-a concentration (Chla) in case 1 ocean waters (Gordon & Morel, 1983; O'Reilly et al., 1998). The absorption and backscattering coefficients are ruled primarily by phytoplankton and its co-varying particulate and dissolved materials(Morel & Prieur, 1977). The spectral behavior of the inherent optical properties (IOPs) of different water components and pure water are relatively well known (Babin et al., 2003; Bricaud et al., 1995; Pope & Fry, 1997), which enables prediction of Chla concentration reasonably well. However, application of such algorithms derived from case 1 waters to case 2 waters results in poor predictability (Zimba & Gitelson, 2006; Dall'Olmo et al., 2005; Lavender et al., 2004) because of overlapping and uncorrelated absorption of dissolved organic matter and tripton. Strong absorption in the blue spectral region by dissolved organic matter, tripton and phytoplankton pigments requires the use of other spectral regions for Chla estimation.

A variety of algorithms have been developed for estimating Chla in turbid waters. All of these algorithms are based on the spectral properties near 700 nm. The widely used variable is the ratio of the near-infrared (NIR) peak reflectance to the reflectance near 675 nm which is the red absorption peak of chlorophyll-a. Gons (1999) and Gons et al. (2000) first derived the backscattering coefficient (b_b) at 704 and 672 nm, and then used the reflectance ratio of 704 nm to 672 nm and absorption at these wavelengths to assess Chla concentration. Jiao et al. (2006) used the reflectance ratio of 719 nm to 667 nm to estimate Chla concentration in Taihu Lake. Thiemann & Kaufman (2000) used the ratio of 705 to 678 nm to assess Chla in Mecklenburg Lake; the reflectance ratio of specific band beyond 725 and 675 nm was also used by other researchers to estimate Chla (Pierson & Sträombäack, 2000; Pulliainen et al., 2001; Dall'Olmo et al., 2005). These algorithms all assume that optical parameters such as Chla specific absorption coefficient and Chla fluorescence quantum yield remain constant, which considerably impacts their accuracy (Dall'Olmo & Gitelson, 2005, 2006). These parameters, in practice, are variable and depend on the physiological and ecological dynamics of the phytoplankton community. For instance, the Chla specific absorption is affected by accessory pigments and "package effect" (Lohrenz et al., 2003; Nelsoń et al., 1993; Bricaud et al., 1995; Mercado et al., 2008). The Chla fluorescence quantum yield depends on several factors, such as phytoplankton taxonomic composition, illumination conditions, nutritional status, and so on (Babin et al., 1996). Because

* Corresponding author.
E-mail address: lcf320@126.com (C. Le).

0034-4257/$ – see front matter.
doi:10.1016/j.rse.2009.02.005

spectral reflectance data were collected under sunlight that provided the excitation energy for Chla fluorescence, the Chla fluorescence signal fills in the reflectance and consequence shifting the reflectance minimum toward shorter wavelengths (Dall'Olmo & Gitelson, 2005).

Alternatively, other algorithms such as fluorescence line height (Fischer & Kronfeld, 1990; Gower et al., 1999), first derivative of reflectance algorithm (Han & Rundquist, 1997; Han, 2005), have also been used to estimate Chla concentration in turbid waters. As for fluorescence line height, quantitative accuracy is limited by the varying populations and by changes in water constituents' absorption that reduces the available light for fluorescence, especially in productive turbid waters with highly variable optical properties, while the first derivative of reflectance algorithm is only able to remove pure water effect (Goodin et al., 1993). While the estimation accuracy of the first derivative algorithm is limited by suspended solids and dissolved matter concentration. These algorithms are inapplicable to productive turbid waters of highly variable optical properties.

Recently, Dall'Olmo & Gitelson (2005) outlined a three-band semi-analytical algorithm for estimating chlorophyll concentration in turbid waters, and described how the algorithm works, and further analyzed the influence factors of the algorithm, as well as suggested a method to optimize the band positions. This model requires reflectance of three spectral bands λ_1, λ_2, and λ_3 in the form of $[\mathrm{Rrs}(\lambda_1)^{-1} - \mathrm{Rrs}(\lambda_2)^{-1}] \times \mathrm{Rrs}(\lambda_3)$. The first band λ_1 should be maximally sensitive to phytoplankton absorption (a_{Chla}), the second band λ_2 minimizes the effect of suspended solids absorption [$a_d(\lambda)$], dissolved matter absorption [$a_{\mathrm{CDOM}}(\lambda)$] and pure water absorption [$a_w(\lambda)$]. The effect of backscattering (b_b) by all particulate matter is minimized by the third band λ_3. This semi-analytical algorithm involves three assumptions: 1) the absorption by suspended solids and CDOM at λ_2 is close to that at λ_1; 2) reflectance at λ_3 is minimally affected by the absorption of water constituents and can only account for the variability in scattering between samples; and 3) the total backscattering coefficient of the three bands is approximately equal. The algorithm has been well validated using *in situ* observations from different lakes and reservoirs with variable optical properties (Zimba & Gitelson, 2006), and Gitelson et al. (2008) demonstrated that the three-band semi-analytical model can be used to assess Chla in various turbid waters without re-parameterization.

It has also been demonstrated that the accuracy of the three-band algorithm is considerably affected by the variability of the quantum yield of Chla fluorescence and the specific absorption coefficient (Dall'Olmo & Gitelson, 2005, 2006), and the influence always varies among specific waters. In order to locate the optimal position of the three-band algorithm, model tuning and accuracy optimization were used by Zimba and Gitelson (2006) to estimate chlorophyll concentrations in hyper-eutrophic aquatic systems, and concluded that $[\mathrm{Rrs}(650)^{-1} - \mathrm{Rrs}(710)^{-1}] \times \mathrm{Rrs}(740)$ could accurately assess Chla concentration. Gitelson et al. (2008) found that estimation RMSE was minimized for λ_1 ranging from 658 to 674 nm, λ_2 between 700 and 735 nm and λ_3 between 733 and 780 nm.

However, the three assumptions for the three-band semi-analytical algorithm may be violated in highly turbid waters. For example, Tzortziou et al. (2006) showed that the absorption of particulate matter in the 700–730 nm region cannot be neglected in the Chesapeake Bay; Tassan and Ferrari (2003) found that the aquatic particle absorption significantly varies with the type of suspended particles. The absorption ranged from negligible to generally significant for natural assemblages of aquatic particles. Similar conditions were also found in the highly turbid waters of Taihu Lake where the high concentration and multi-sourced suspended matter cause non-negligible absorption in the NIR region. The amount of absorption by suspended solids is occasionally comparable to that of Chla in the red region at low Chla concentration levels. Furthermore, the backscattering coefficient is always comparable to total absorption in highly turbid waters. Thus, it is significant to validate the applicability of the three-band algorithm in Taihu Lake, and improve the performance of the three-band algorithm by minimizing the effect of suspended solid absorption in the NIR region.

The objective of this study is to validate the three-band semi-analytical algorithm and further improve it for Taihu Lake. The specific goals are: (1) to locate the optimal spectral positions of the three bands; (2) to evaluate the accuracy of the three-band semi-analytical algorithm for accurately estimating Chla in Taihu Lake; (3) to improve the performance of the three-band algorithm by developing a four-band semi-analytical algorithm; and (4) to compare the accuracy of the three-band and four-band models in estimating Chla in highly turbid and productive waters of Taihu Lake.

2. Study area

Taihu Lake is the third largest freshwater lake in China located between 30°56′–31°33′ N and 119°553′–120°536′ E. It has a water area of 2338 km^2 and a mean depth of 1.9 m. Since the 1980s rapid industrialization and urbanization in the surrounding urban areas, in conjunction with the widespread use of fertilizers in the rural areas have produced an enormous amount of wastewater and sewage discharged into the lake without treatment. The nutrient concentration in the lake has been on incessant rise since then. Consequently, water eutrophication has becoming a serious environmental problem that threatens the normal functioning of lake life. For instance, the accumulation of cyanobacteria *Microcystis* spp. has brought out disastrous algal blooms that disrupted the normal operation of the water plants and complete shutdown of the water supply system for major cities along the lakeshore. The density of cyanobacteria is particularly high from May to October each year. The algal blooms are also potentially hazardous to the health of the people living in the lake area through the consumption of contaminated aquatic products. It is thus importance to estimate Chla concentration timely to predict the outbreak of algal blooms by means of remote sensing.

Taihu Lake is selected for the study because the water of the lake is highly turbid. It is difficult to estimate Chla concentration accurately for this lake because the optical properties of the water constituents undergo great spatiotemporal change (Zhang et al., 2007; Le et al., 2009). The absorption signal of phytoplankton is partly overwhelmed by that of suspended solid absorption and backscattering. It is difficult to estimate chlorophyll concentration accurately by using conventional algorithms such as band ratio and the first differential algorithm.

3. Materials and methods

3.1. Datasets used

Two datasets were collected in this study. The first contains 52 samples of optical properties and concentration of water constituents, the optical properties contained total absorption of suspend sediment, non-algal particle, phytoplankton and colored dissolvable organic matter (CDOM), and water constituents contained concentrations of suspended sediment and chlorophyll. This dataset recorded from 8 to 22 November of 2007 was used to calibrate and improve the three-band algorithm. The second dataset contains 80 samples of hyperspectral reflectance and Chla concentration that ranges from 4 to 158 mg m^{-3}. It was used to assess the accuracy of the two algorithms. It was collected in five field trips spanning over a period of three days in each month from early June to early October 2005.

3.2. Field measurements

Water samples and reflectance measurements were collected between 10:00 and 14:00 h local time. Surface water samples (2.5 L

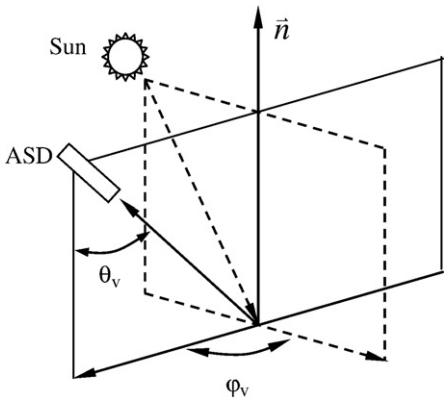

Fig. 1. Viewing geometry of the above-water measurement.

volume) were collected at a depth of 0.5 m below the surface immediately after reflectance measurement. The samples were stored in a cooler with ice in the dark, and taken back to the laboratory for analyzing concentration of Chla, total suspended solid (TSS) and absorption coefficient at the end of the day.

Hyperspectral reflectance measurements took place in a boat using ASD FieldSpec Spectroradiometer. With a field view of 25°, this instrument has a sensitivity range from 350 to 1050 nm at an increment of 1.5 nm with 512 bands. The resolution was transformed into 1 nm by the interior software. During measurement the instrument was hand-held over the deck of an anchored ship approximately 1 m above the water surface. Radiance was measured of both the water surface (L_{sw}) and a standard gray board (L_p). Ten curves were acquired for each target. In order to effectively avoid the interference of the ship with the water surface and the influence of direct solar radiation, the instrument was positioned at an angle φ_v of 90–135° with the plane of the incident radiation away from the sun (Fig. 1). The view of the water surface was controlled between 30 and 45° with the aplomb direction. In this way most of the direct sunlight was eliminated while the impact of the ship's shadow was minimized. Immediately after measuring water radiance, the spectroradiometer was rotated upwards by 90–120° to measure skylight radiance (L_{sky}). The view zenith angle in this measurement was kept the same as that in measuring water radiance. Hyperspectral reflectance is computed as:

$$R_{rs} = L_w / E_d\left(0^+\right) \tag{1}$$

where L_w is the water-leaving radiance, $E_d(0^+)$ is the total incident radiant flux of the water surface.

L_w and $E_d(0^+)$ in Eq. (1) is further calculated as:

$$L_w = L_{sw} - rL_{sky} \tag{2}$$

where L_{sw} stands for total radiance received from the water surface; L_{sky} refers to diffused radiation of the sky, which contains no information on water properties, and hence has to be eliminated; r represents the reflectance of the skylight at the air–water interface (Mobley, 1999). Its value depends upon solar azimuth, measurement geometry, wind speed, and surface roughness.

$$E_d\left(0^+\right) = \pi L_p / \rho_p \tag{3}$$

where L_p is the radiance of the gray board, ρ_p stands for the reflectance of the gray board, which has been accurately calibrated to 30%.

Reflectance measurement followed the Ocean Optical Protocols (Revision 3) by NASA (2002). Reflectance was measured in the sunny side of the boat when the wind speed was less than 2.5 $m \cdot s^{-1}$. During sampling the water was so turbid that light could not penetrate through it to reach the lake bottom, so bottom reflectance was irrelevant in the measured water surface reflectance. Spectral measurements of absorption by water constituents were carried out for the validation dataset using Shimadzu UV-2550 PC UV–Vis spectrophotometer. The total particle material absorption[$a_p(\lambda)$], non-phytoplankton particles absorption [$a_d(\lambda)$] and phytoplankton absorption[$a_{ph}(\lambda)$] were determined by the quantitative filter technique(QFT) (Mitchell, 1990). Water samples (50–200 ml) were collected and filtered onto a 47 mm diameter Whatman fiberglass GF/F filter under low vacuum pressure. For more details, refer to Le et al. (2009).

3.3. Laboratory analyses

Pigment samples were extracted in hot (80 °C) 90% ethanol, and Chla concentration was quantified fluorometrically (Welschmeyer, 1994). The concentration of TSS, organic suspended solids (OSS), and inorganic suspended solids (ISS) were determined gravimetrically. Samples were filtered through pre-combusted Whatman GF/F filters (550 °C for 4 h) to remove dissolved organic matter in suspension, which was then dried (105 °C for 4 h) and weighed to obtain TSS. The filters were re-combusted at 550 °C for 4 h, and weighted again to obtain ISS. Subtraction of ISS from TSS resulted in OSS.

3.4. Accuracy assessment

In order to find out the optimal positions of the bands in the semi-analytical model, the resulting standard error of Chla estimation (STE) was calculated using Eq. (4) for the validation dataset iteratively from 400 nm to 750 nm, as suggested by Dall'Olmo and Gitelson (2006).

$$\mathrm{STE} = \left[\sum\left(\mathrm{Chla}_{\mathrm{measurement},i} - \mathrm{Chla}_{\mathrm{predicted},i}\right)^2 / (N/2)\right]^{0.5} \tag{4}$$

where $\mathrm{Chla}_{\mathrm{measurement}}$ is the concentration measured in laboratory, $\mathrm{Chla}_{\mathrm{predicted}}$ represents the concentration predicted from the retrieval models, i is the band wavelength, $N-2$ is the degree of freedom.

The accuracy of the two algorithms was then assessed by calculating the relative error (RE) using the following equation:

$$\mathrm{RE} = \left[100 \times \left|\mathrm{Chla}_{\mathrm{measurement}} - \mathrm{Chla}_{\mathrm{predicted}}\right| / \mathrm{Chla}_{\mathrm{measurement}}\right]\% \tag{5}$$

The mean relative errors (MRE) and root mean squire error (RMSE) were also calculated in this study to assess the performance of the two algorithms.

Table 1
Descriptive statistics of the measured optical properties and concentration of water constituents.

	Max	Min	Median	Average	SD
TSS($mg \cdot L^{-1}$)	213.60	8.53	24.13	38.21	35.56
OSS($mg \cdot L^{-1}$)	29.53	3.73	8.33	9.50	4.37
ISS($mg \cdot L^{-1}$)	195.20	2.60	13.47	28.71	33.78
Chla($\mu g \cdot L^{-1}$)	89.23	0.98	11.07	16.49	17.14
$a_{CDOM}(440)(m^{-1})$	1.42	0.02	0.39	0.46	0.31
$a_d(440)(m^{-1})$	7.16	0.57	0.81	2.32	1.73
$a_{ph}(440)(m^{-1})$	9.37	0.21	0.36	1.35	1.74
$a_{ph}(675)(m^{-1})$	3.99	0.06	1.62	0.53	0.69

TSS, total suspended solids; ISS, inorganic suspended solids; OSS, organic suspended solids; Chla, chlorophyll a concentration; $a_{CDOM}(440)$, absorption coefficient of CDOM at 440 nm; $a_d(440)$, non-algal particles absorption coefficient at band 440 nm; $a_{ph}(440)$, absorption coefficient of phytoplankton at band 440 nm, while $a_{ph}(675)$ stand for absorption at band 675 nm; SD is the standard deviation of those parameters.

4. Results

4.1. Constituent concentrations and composition

The dataset used to validate the three-band algorithm encompasses widely varying optical conditions and constituents concentration (Table 1). TSS concentration is very high at an average of 38.2 $mg \cdot L^{-1}$. Hence, Taihu Lake water is extremely turbid. Chla concentration ranges from 0.98 to 89.23 $\mu g \cdot L^{-1}$, the average being 16.49 $\mu g \cdot L^{-1}$. The high Chla concentration indicates that Taihu Lake has been severely eutrophied. The poor correlation between TSS and Chla (correlation coefficient $r = 0.3$, $p < 0.001$) clearly indicates that Chla is not the only contributor of water optical properties, and Taihu Lake water falls into the case 2 category.

Owing to a wide range of constituent concentration, the dataset also shows large variations in optical properties. The absorption of non-algal particles at 440 nm ranges from 0.57 to 7.16 m^{-1}, with an average of 2.32 m^{-1}. The phytoplankton absorption coefficient at 675 nm ranges from 0.06 to 3.99 m^{-1} (average = 0.53 m^{-1}). Similar to the absorption coefficient, the specific absorption of phytoplankton also varies widely. The specific absorption of phytoplankton at 675 nm ranges from 0.006 to 0.057 $m^2\ mg^{-1}$, with an average value of $0.021 \pm 0.011\ m^2\ mg^{-1}$.

4.2. Spectral reflectance properties

Spectral reflectance over the visible and NIR regions exhibits a large variability in the two datasets. The magnitude and shape of the reflectance curves (Fig. 2) are all similar to that of typical turbid water (Gitelson et al., 2008). The reflectance in the blue range (400–500 nm) is relative low owing to high absorption by water constituents. However, the reflectance spectral feature of Taihu Lake water in this region is not prominent because of widely ranging TSS and Chla concentration.

Reflectance in the red region (600–700 nm) has several spectral features. Water containing blue–green algae has a slight reflectance trough around 620 nm formed by the secondary absorption peak by phycocyanin in this region (Simis et al., 2005). A second reflectance trough around 675 nm corresponds to the red Chla absorption. However, the reflectance around 675 nm is poorly correlated with Chla concentration (value of r is −0.07), an outcome of absorption and scattering by other constituents.

A distinct peak around 700 nm appears in almost all reflectance curves. The peak shifts from 690 nm at low Chla to 715 nm at high Chla. Because of the low chlorophyll and high suspended sediments, the peak of some reflectance curves in this region is feeble. This peak results from both high backscattering and minimum absorption by all optically active constituents, including pure water.

4.3. Algorithm calibration and evaluation

4.3.1. Three-band algorithm calibration

Band tuning and accuracy optimization (Zimba & Gitelson, 2006; Dall'Olmo & Gitelson, 2006) were used in this study to find the approximate positions for λ_1, λ_2 and λ_3 in the three-band algorithm. To find the optimal λ_1, initial position for λ_2 was set to 700 nm within the reflectance peak range. The initial position for λ_3 was set to 750 nm at which the reflectance is contributed mainly by particulate backscattering and pure water absorption. As λ_1 was tuned from 400 to 750 nm, the STE of $[Rrs^{-1}(\lambda_1) - Rrs^{-1}(710)]Rrs(750)$ versus Chla was calculated (Fig. 3a). STE varies with wavelength λ_1, its minimum occurs at 660 nm. Thus 660 nm was selected for λ_1.

To determine the optimal position of λ_2, $\lambda_1 = 690$ nm and $\lambda_3 = 750$ nm was used, and λ_2 was tuned from 400 to 750 nm. The STE of model $[Rrs^{-1}(660) - Rrs^{-1}(\lambda_2)]Rrs(750)$ versus Chla was again computed for each λ_2. The result (Fig. 3b) indicates that minimum STE exists at 692 nm. Thus, this wavelength was selected for λ_2.

The optimal λ_3 was determined by setting $\lambda_1 = 660$ nm and $\lambda_2 = 692$ nm, and the minimum STE occurs at 740 nm. In order to assess whether 660 nm is optimal, the optimal position of λ_1 was redetermined by setting $\lambda_2 = 692$ and $\lambda_3 = 740$ nm, and the result shows that the minimum STE was at 660 nm. Thus, the model $[Rrs^{-1}(660) - Rrs^{-1}(692)]Rrs(740)$ should be used as it has the minimum STE value of 5.65 $mg\ m^{-3}$.

4.3.2. Construction of the four-band model

As the absorption of suspended solids is non-negligible and the backscattering is significant in the NIR spectrum in highly turbid waters, and the high absorption of pure water in the NIR region also affects the accuracy of the three-band algorithm, a four-band semi-analytical algorithm was developed to improve the performance of the three-band algorithm. The improvement is achieved by subtracting the effect of suspended solids and minimizing the effect of pure water absorption as well as backscattering in the NIR region.

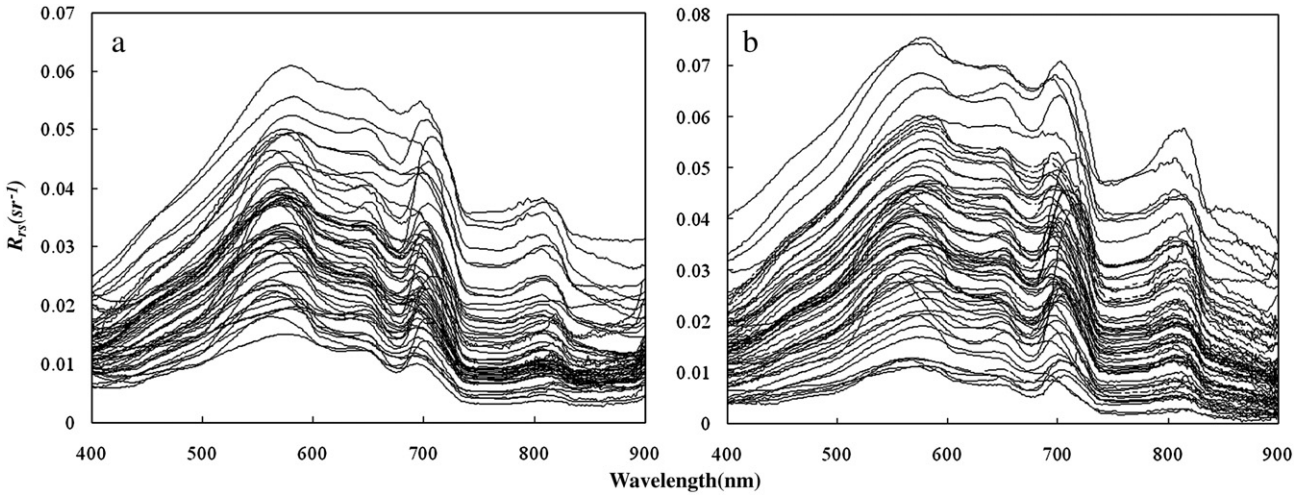

Fig. 2. Remote sensing reflectance spectra of Taihu Lake. (a) Reflectance of the calibration dataset collected during 8–27 November, 2007. (b) Reflectance of the evaluation dataset collected from June to October of 2005.

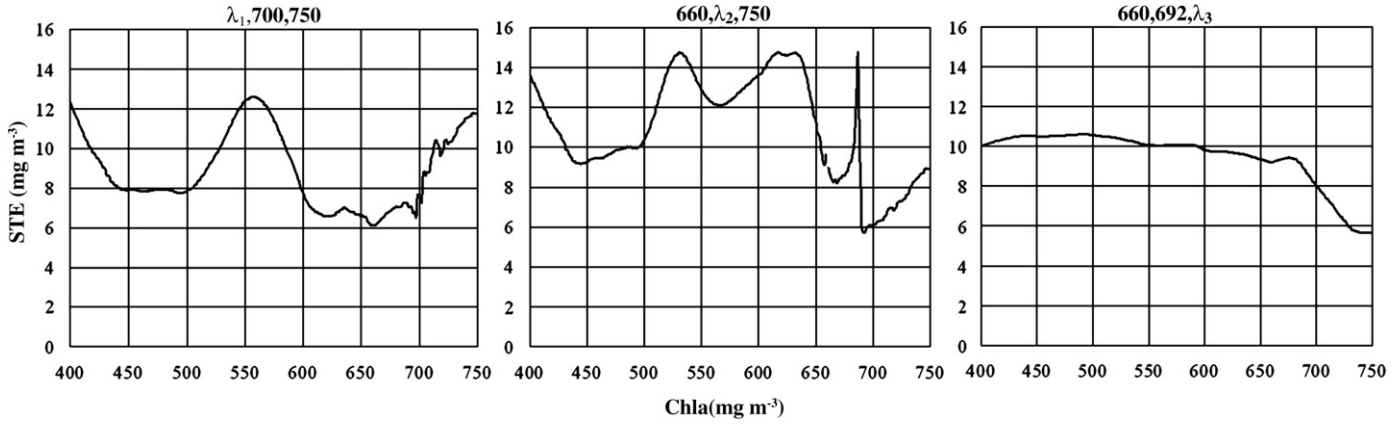

Fig. 3. STE of estimate resulting from regressing different model versions versus measured Chla: (a) $[Rrs^{-1}(\lambda_1) - Rrs^{-1}(700)]Rrs(750)$ letting vary λ_1; (b) $[Rrs^{-1}(660) - Rrs^{-1}(\lambda_2)]Rrs(750)$ letting vary λ_2 and (c) $[Rrs^{-1}(660) - Rrs^{-1}(692)]Rrs(\lambda_3)$ letting vary λ_3.

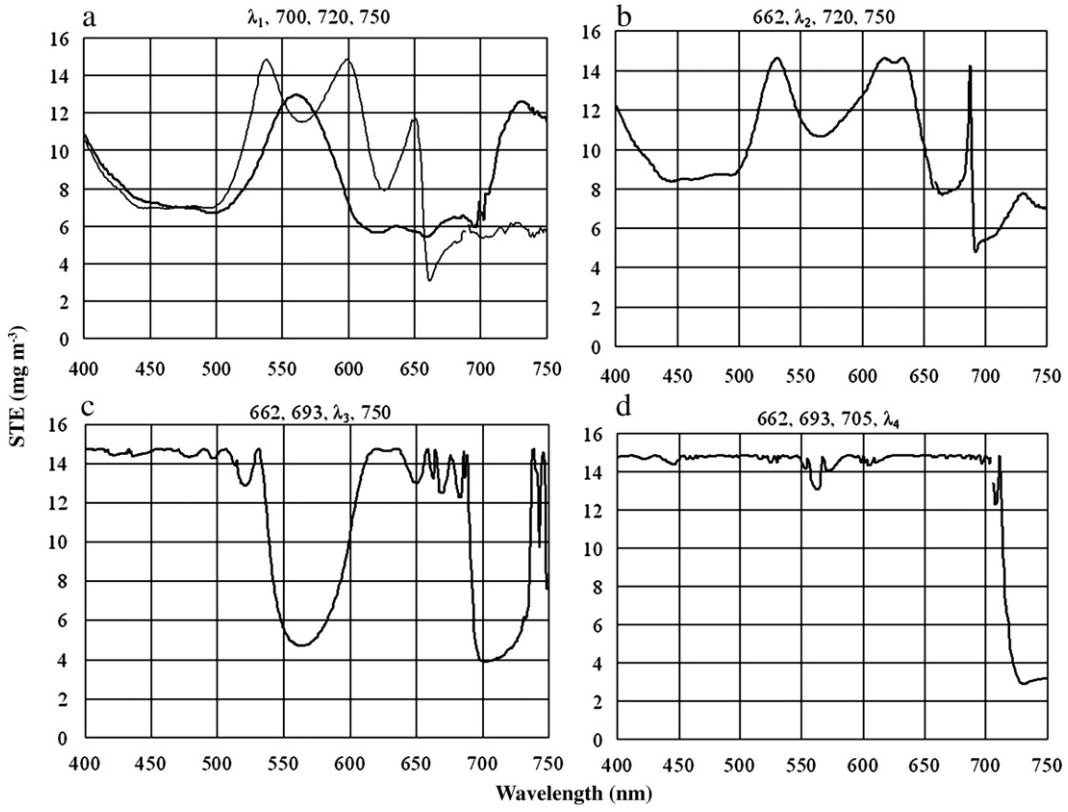

Fig. 4. STE of Chla from various regression models versus measured Chla at different wavelengths. (a)$[Rrs^{-1}(\lambda_1) - Rrs^{-1}(700)][Rrs^{-1}(750) - Rrs^{-1}(720)]^{-1}$ (thick line); $[Rrs^{-1}(\lambda_1) - Rrs^{-1}(693)][Rrs^{-1}(740) - Rrs^{-1}(705)]^{-1}$ (thin line); (b)$[Rrs^{-1}(662) - Rrs^{-1}(\lambda_2)][Rrs^{-1}(750) - Rrs^{-1}(720)]^{-1}$; (c) $[Rrs^{-1}(662) - Rrs^{-1}(693)][Rrs^{-1}(750) - Rrs^{-1}(\lambda_3)]^{-1}$ and (d) $[Rrs^{-1}(662) - Rrs^{-1}(693)][Rrs^{-1}(\lambda_4) - Rrs^{-1}(705)]^{-1}$.

The four-band algorithm is derived by replacing $Rrs(\lambda_3)$ in the three-band algorithm with $[Rrs^{-1}(\lambda_4) - Rrs^{-1}(\lambda_3)]^{-1}$, and is written as $[Rrs^{-1}(\lambda_1) - Rrs^{-1}(\lambda_2)][Rrs^{-1}(\lambda_4) - Rrs^{-1}(\lambda_3)]^{-1}$. The three-band algorithm based on the three assumptions described above can be expressed as:

$$\left[Rrs^{-1}(\lambda_1) - Rrs^{-1}(\lambda_2)\right] * Rrs(\lambda_3) = [a_{chla}(\lambda_1) + a_w(\lambda_1) - a_w(\lambda_2)] / a_w(\lambda_3) \quad (6)$$

But, if the absorption and backscattering of suspended solids at λ_3 is non-negligible, the three-band algorithm should be re-written as:

$$\left[Rrs^{-1}(\lambda_1) - Rrs^{-1}(\lambda_2)\right] * Rrs(\lambda_3) = [a_{chla}(\lambda_1) + a_w(\lambda_1) - a_w(\lambda_2)] / [a_w(\lambda_3) + b_b + a_d(\lambda_3)] \quad (7)$$

The four-band model was established by replacing the $Rrs(\lambda_3)$ term in the three-band algorithm by $[Rrs^{-1}(\lambda_4) - Rrs^{-1}(\lambda_3)]^{-1}$. It is expressed as:

$$\left[Rrs^{-1}(\lambda_1) - Rrs^{-1}(\lambda_2)\right]\left[Rrs^{-1}(\lambda_4) - Rrs^{-1}(\lambda_3)\right]^{-1} = [a_{chla}(\lambda_1) + a_w(\lambda_1) - a_w(\lambda_2)] / [a_w(\lambda_4) - a_w(\lambda_3)] \quad (8)$$

Compared to Eq. (2), this model removes the absorption and backscattering of suspended solids over the NIR region, and minimizes pure water absorption.

The optimal position of the four bands was determined via band tuning and accuracy optimization as described previously (Zimba & Gitelson, 2006; Dall'Olmo & Gitelson, 2006). For instance, the initial

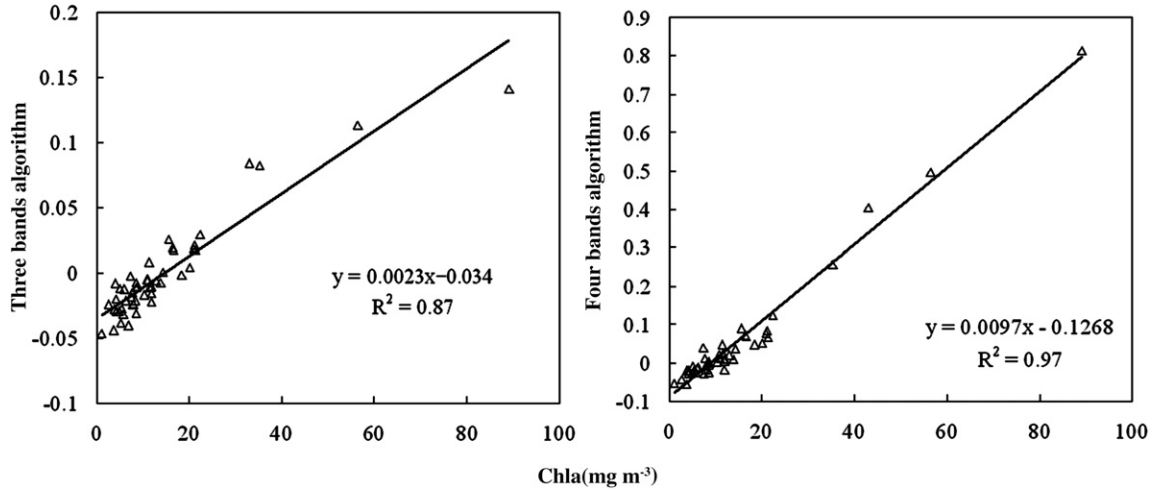

Fig. 5. Scatterplot of estimated versus measured Chla concentrations of 2007 using two algorithms. (a) Results from the three-band algorithm; (b) Results from the four-band model.

position for $\lambda_2 = 700$ nm, $\lambda_3 = 720$ nm and $\lambda_4 = 750$ nm was used to determine λ_1. The STE of $[Rrs^{-1}(\lambda_1) - Rrs^{-1}(700)][Rrs^{-1}(750) - Rrs^{-1}(720)]^{-1}$ versus Chla concentration varies with wavelength over 400–750 nm (Fig. 4a). At 662 nm STE reaches the minimum value of 5.44 mg m^{-3}. This value is smaller than the corresponding figure (5.65 mg m^{-3}) in the above three-band algorithm. Thus, 662 nm was selected for λ_1.

Similarly, optimal position of λ_2 was determined by setting $\lambda_1 =$ 662 nm, $\lambda_3 = 720$ nm and $\lambda_4 = 750$ nm. The minimum STE of 4.93 mg m^{-3} appears at 693 nm (Fig. 4b). Then, $\lambda_1 = 662$ nm, $\lambda_2 = 693$ nm and $\lambda_4 = 750$ were used to find the optimal λ_3. STE becomes minimum (3.86 mg m^{-3}) at 705 nm (Fig. 4c). Thus, 705 nm was selected for λ_3 while 662 nm and 705 nm were selected for λ_1 and λ_2, respectively. Fig. 4d shows the STE results of band tuning. Minimum STE lies in the range of 730–740 nm, with a value between 2.9 and 3.1 mg m^{-3}. The optimal bands were assessed by redetermining the optimal position of λ_1 using $\lambda_2 = 693$ nm, $\lambda_3 = 705$ nm and $\lambda_4 = 740$ nm. Results show that the redetermined optimal position forλ_1 lies at 663 nm (the thin line in Fig. 4a where STE has a value of 2.9 mg m^{-3}. Thus, the four-band algorithm has the optimal accuracy in case of $\lambda_1 = 663$ nm, $\lambda_2 = 693$ nm, $\lambda_3 = 705$ nm and $\lambda_4 = 740$ nm.

4.4. Accuracy evaluation

The performance of the three-band and four-band models was evaluated by examining their respective mean relative error (MRE)

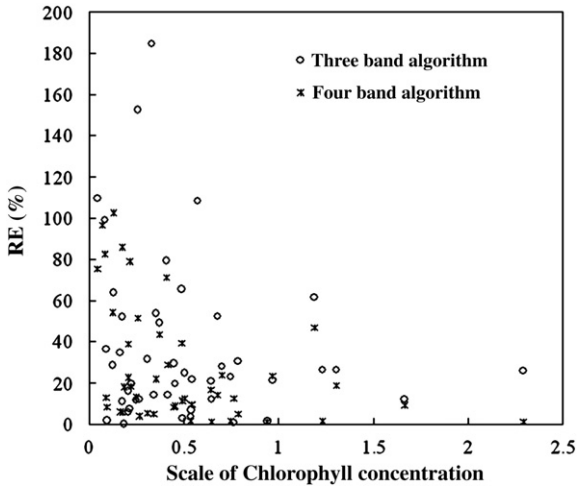

Fig. 6. The relationship between RE and the scale of chlorophyll concentration.

in estimating Chla. Fig. 5 shows the relationship between Chla modeled from $[Rrs^{-1}(660) - Rrs^{-1}(692)]Rrs(740)$ and $[Rrs^{-1}(662) - Rrs^{-1}(693)][Rrs^{-1}(740) - Rrs^{-1}(705)]^{-1}$, and measured Chla in the 2007 dataset. Both models produced good predictions of Chla, but the four-band model has a superior performance to the three-band one. Use of the four-band model in estimating Chla concentration in Taihu Lake decreases the uncertainty of estimation by 17% from the three-band model, and the RMSE (root mean squire error) also decreases from 5.35 mg m^{-1} of three-band algorithm to 2.49 mg m^{-1} of four-band algorithm.

The relationship between RE and the scale of chlorophyll a concentration (Chla/TSS) was also presented to demonstrate the ability of the two algorithms in estimating chlorophyll a. Fig. 6 shows a plot of chlorophyll concentration versus RE of the two algorithms. It illustrates that RE decreases with increasing chlorophyll a concentration, but there is no statistically significant relationship between them. That is to say, both bands are capable of the estimation in highly turbid waters. Comparison of the RE value of the four-band algorithm (tagged by star) to that of the three-band algorithm (tagged by circle) reveals that the four-band algorithm considerably reduces the RE value and outperforms the three-band algorithm, especially at a low chlorophyll concentration level.

The stability and performance of the two models were further evaluated using the independent 2005 dataset. Both models allow Chla concentration to be predicted quite accurately (Fig. 7). They account for more than 80% variation in Chla concentration, and hence can be used to accurately estimate Chla in highly turbid waters of Taihu Lake. The estimation accuracy is significant improved with the use of the four-band model. It accounts for nearly 10% more variation in Chla concentration than the three-band model while reducing the MRE of the estimate by over 6%. The RMSE was 9.74 mg m^{-1} of the four-band algorithm versus 12.76 mg m^{-1} of the three-band algorithm. Therefore, the four-band model is more accurate than the three-band model in estimating Chla concentration in highly turbid Taihu Lake waters.

5. Discussion

The optimal positions of the three bands determined in this study are consistent with the findings of other researchers. Gitelson et al. (2008) found that the RMSE is minimized by fixing the position of λ_1 over the 658–674 nm range, λ_2 over the 700–735 nm range, and λ_3 over a wide range between 733 and 780 nm. In the case of the Chesapeake Bay, the minimal RMSE was achieved by $\lambda_1 = 674$–676 nm, $\lambda_2 = 691$–698 nm and $\lambda_3 = 723$–739 nm (Gitelson et al., 2007). In estimating widely ranging Chla concentrations, Zimba and

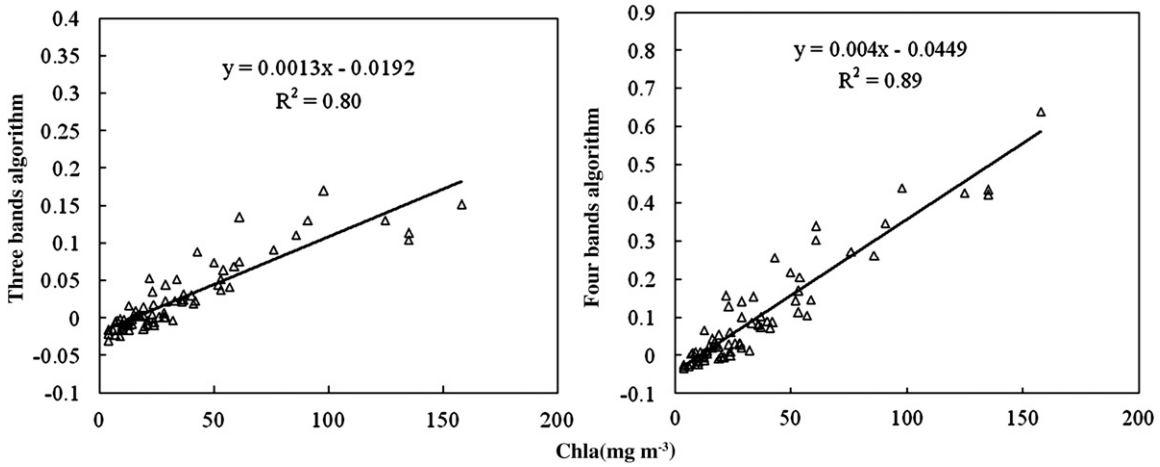

Fig. 7. Scatterplots of the Chla levels estimated using the three-band (a) and four-band (b) model versus the measured Chla concentrations using the 2005 dataset.

Gitelson (2006) found that the minimal RMSE is achieved using the optimal positions of $\lambda_1 = 650$ nm, $\lambda_2 = 710$ nm and $\lambda_3 = 740$ nm.

These findings demonstrate that the optimal position of the three bands always lies within a wavelength range. Their specific value varies with water constituents and their optical properties, especially the Chla fluorescence quantum yield and the Chla specific absorption coefficient (Dall'Olmo & Gitelson, 2005, 2006). These two are the main optical properties that degrade the estimation accuracy. Other factors include water absorption (Gitelson et al., 2008). Strong absorption by water in the NIR greatly reduces the intensity of the recorded signal in the NIR region, and consequently the signal-to-noise ratio, and enhances the effect of inherent noise in the recorded signal. Furthermore, the three-band algorithm is based on the assumption that the absorption by water constituents is negligible in the NIR regions and the absorption is much higher than backscattering (Dall'Olmo & Gitelson, 2005; Gitelson, et al., 2008).

In order to overcome the limitation of the three-band algorithm, a four-band algorithm was developed. In the three-band algorithm, $Rrs^{-1}(\lambda_1) - Rrs^{-1}(\lambda_2)$ was used to minimize the effect of suspended solids and CDOM, and $Rrs(\lambda_3)$ was used to minimize the backscattering of water constituents. While in the four band algorithm, $[Rrs^{-1}(\lambda_4) - Rrs^{-1}(\lambda_3)]^{-1}$ was used to minimize the effect of high absorption of pure water and non-negligible absorption of suspended solids in the NIR region, as well as reduce the effects variable backscattering of water constituents in this study. As a consequence, the signal of Chla was extruded and the signal-to-noise ratio enhanced, particularly at low Chla concentration levels. Thus, $Rrs(\lambda_3)$ in the three-band algorithm was replaced by $[Rrs^{-1}(\lambda_4) - Rrs^{-1}(\lambda_3)]^{-1}$ and a four-band model was developed.

Comparison shows that the measured values much more closely resemble the retrieved Chla using the four-band algorithm than its three-band counterpart (Figs. 4 and 5) with an improved accuracy of estimation, even at low Chla concentration. The four-band model achieved an MRE of 37.1%, against 63.6% of the three-band algorithm at Chla concentration below 10 mg m^{-3}. For the dataset of 2005, the MRE of the four-band algorithm is 32.6%, lower than 48.4% for the three-band algorithm at Chla concentration less than 20 mg m^{-3}. The large pace of improvement in the estimation accuracy at low concentration levels is attributed to the removal of the absorption effect of suspended solids in the NIR region and the weakened effect of pure water.

The four-band algorithm is limited in that it is able to suppress the effect of water absorption instead of eradicating it completely. Thus, strong water absorption inevitably exerts a residual effect on the estimation accuracy. Furthermore, other factors such as different illumination conditions and surface water roughness were not taken into consideration in this study, which may degrade the accuracy of the four-band algorithm. It is also notable that the equations used for the two dataset to estimate chlorophyll a has great difference and more study is required to understand it.

6. Summary

In this study two semi-analytical models for estimating Chla concentration were constructed by specifying the optimal wavelengths. The three bands have the optimal wavelengths of $\lambda_1 = 660$ nm, $\lambda_2 = 692$ and $\lambda_3 = 740$ nm. The specification of the wavelength in the four-band model takes the form of $\lambda_1 = 663$ nm, $\lambda_2 = 693$ nm, $\lambda_3 = 705$ nm and $\lambda_4 = 740$ nm. Evaluated using two independently collected datasets in Taihu Lake, China, the three-band semi-analytical algorithm is found to have an acceptable performance in estimating Chla concentration. By comparison, the four-band algorithm has a better performance, even though both models can account for 87% or more variation in Chla concentration. The four-band model explains almost 10% additional variation in Chla concentration than the three-band model. It achieved an MRE of 37.1%, against 63.6% of the three-band algorithm at Chla concentration below 10 mg m^{-3}. At Chla concentration below 20 mg m^{-3} the four-band algorithm has an MRE value of 32.6%, lower than 48.4% for the three-band algorithm. The significantly reduced uncertainty in Chla estimation is due to removal of absorption effect of suspended solids and partial suppression of the effect of water absorption. Thus, they are accurate enough for estimating Chla in the study area that has widely ranging concentration levels of water constituents and their optical properties. It is concluded that the four-band algorithm should be used for estimating Chla concentration in highly turbid case 2 waters, even though it may be essential to reposition the wavelength of the four bands for the given study area accordingly.

Acknowledgements

Funding for this study was received from the Research Plan Foundation from the Ministry of Science and Technology of China (No. 2008BAC34B05); National Science Foundation for Young Scholars of China (No. 40701136); Scientific Research Foundation of Outstanding doctoral of Nanjing Normal University (No. 181200000223); Scientific Research Foundation of Creative Plan for graduate students of Jiangsu Province (No. CX08B_014Z); Scientific Research Foundation for Returned Scholars of Nanjing Normal University (No. 2007105XLH0039) and Ministry of Education (No. [2007]1108); National Natural Science Foundation of China (No. 40571110). We would like to just express our gratitude to Dr. Jay Gao for checking the English language, and the two anonymous reviewers for their useful comments and suggestions.

References

Babin, M., Morel, A., & Gentili, B. (1996). Remote sensing of sea surface sun-induced chlorophyll fluorescence: Consequences of natural variations in the optical characteristics of phytoplankton and the quantum yield of chlorophyll a fluorescence. *International Journal of Remote Sensing*, *17*, 2417–2448.

Babin, M., Stramski, D., Ferrari, G. M., Claustre, H., Bricaud, A., Obolensky, G., & Hoepffner, N. (2003). Variations in the light absorption coefficients of phytoplankton, non-algal particles, and dissolved organic matter in coastal waters around Europe. *Journal of Geophysical Research*, *108*(C7), 1–20.

Bricaud, A., Babin, M., Morel, A., & Claustre, H. (1995). Variability in the chlorophyll-specific absorption coefficients of natural phytoplankton: Analysis and parameterization. *Journal of Geophysical Research*, *100*, 13,321–13,332.

Dall'Olmo, G., & Gitelson, A. A. (2005). Effect of bio-optical parameter variability on the remote estimation of chlorophyll-a concentration in turbid productive waters: Experimental results. *Applied Optics*, *44*(3), 412–422.

Dall'Olmo, G., & Gitelson, A. A. (2006). Effect of bio-optical parameter variability and uncertainties in reflectance measurements on the remote estimation of chlorophyll-a concentration in turbid productive waters: Modeling results. *Applied Optics*, *45*(15), 3577–3592.

Dall'Olmo, G., Gitelson, A. A., Rundquist, D. C., Leavitt, B., Barrow, T., & Holz, J. C. (2005). Assessing the potential of SeaWiFS and MODIS for estimating chlorophyll concentration in turbid productive waters using red and near-infrared bands. *Remote Sensing of Environment*, *96*, 176–187.

Fischer, J., & Kronfeld, V. (1990). Sun-stimulated chlorophyll fluorescence: 1. Influence of oceanic properties. *International Journal of Remote Sensing*, *11*, 2125–2147.

Gitelson, A. A., Dall'Olmo, G., Moses, W. M., Rundquist, D. C., Barrow, T., Fisher, T. R., Gurlin, D., & Holz, J. (2008). A simple semi-analytical model for remote estimation of chlorophyll-a in turbid waters: Validation. *Remote Sensing of Environment*, *112*(9), 3582–3593.

Gitelson, A. A., Schalles, J. F., & Hladil, C. M. (2007). Remote chlorophyll-a retrieval in turbid, productive estuaries: Chesapeake Bay case study. *Remote Sensing of Environment*, *109*, 464–472.

Gons, H. J. (1999). Optical teledetection of chlorophyll a in turbid inland waters. *Environment Science & Technology*, *33*, 1127–1132.

Gons, H. J., Rijkeboer, M., Bagheri, S., & Ruddick, K. G. (2000). Optical teledetection of chlorophyll a in estuarine and coastal waters. *Environmental Science & Technology*, *34*, 5189–5192.

Goodin, D., Han, L., Fraser, R., Rundquist, D., & Stebbins, W. (1993). Analysis of suspended solids in water using remotely sensed high resolution derivative spectra. *Photogrammetric Engineering and Remote Sensing*, *59*, 505–510.

Gordon, H., & Morel, A. (1983). Remote assessment of ocean color for interpretation of satellite visible imagery. *A Review. Lecture notes on Coastal and Estuarine Studies* (pp. 114). New York: Springer-Verlag.

Gower, J. F. R., Doerffer, R., & Borstad, G. A. (1999). Interpretation of the 685 nm peak in water-leaving radiance spectra in terms of fluorescence, absorption and scattering, and its observation by MERIS. *International Journal of Remote Sensing*, *20*, 1771–1786.

Han, L. H. (2005). Estimating chlorophyll-a concentration using first-derivative spectra in coastal water. *International Journal of Remote Sensing*, *26*(23), 5235–5244.

Han, L. H., & Rundquist, D. C. (1997). Comparison of NIR/RED ratio and first derivative of reflectante in estimating algal–chlorophyll concentration: A case study in a turbid reservoir. *Remote Sensing of Environment*, *62*, 253–261.

Jiao, H. B., Zha, Y., Gao, J., Li, Y. M., Wei, Y. C., & Huang, J. Z. (2006). Estimation of chlorophyll-a concentration in Lake Tai, China using in situ hyperspectral data. *International Journal of Remote Sensing*, *27*(19), 4267–4276.

Lavender, S. J., Pinkerton, M. H., Froidefond, J. M., Morales, J., Aiken, J., & Moore, G. F. (2004). SeaWIFS validation in European coastal waters using optical and biogeochemical measurements. *International Journal of Remote Sensing*, *25*, 1481–1488.

Le, C. H., Li, Y. M., Zha, Y., & Sun, D. Y. (2009). Specific absorption coefficient and the phytoplankton package effect in Lake Taihu, China. *Hydrobiologia*, *619*, 27–37.

Lohrenz, S. E., Weidemann, A. D., & Merritt, T. (2003). Phytoplankton spectral absorption as influenced by community size structure and pigment composition. *Journal of Plankton Research*, *25*(1), 35–61.

Mercado, J. M., Ramírez, T., & Corté, D. (2008). Changes in nutrient concentration induced by hydrological variability and its effect on light absorption by phytoplankton in the Alborán Sea (Western Mediterranean Sea). *Journal of Marine Systems*, *71*(1-2), 31–45.

Mitchell, B. G. (1990). Algorithms for determining the absorption coefficient of aquatic particulates using the quantitative filter technique (QFT). *SPIE*, *1302*, 137–148.

Mobley, C. D. (1999). Estimation of the remote sensing reflectance from above-surface measurements. *Applied Optics*, *38*, 7442–7455.

Morel, A., & Prieur, L. (1977). Analysis of variations in ocean color. *Limnology and Oceanography*, *22*, 709–722.

Nelsoń, N. B., Prézelin, B. B., & Bidigare, R. R. (1993). Phytoplankton light absorption and the package effect in effect in California coastal waters. *Marine Ecology. Progress Series*, *94*, 217–227.

O'Reilly, J., Maritorena, S., Mitchell, B. G., Siegel, D., Carder, K. L., Garver, S., Kahru, M., & McClain, C. (1998). Ocean color chlorophyll algorithms for SeaWIFS. *Journal of Geophysical Research*, *103*, 24937–24953.

Pierson, D., & Sträombäack, N. (2000). A modeling approach to evaluate preliminary remote sensing algorithms: Use of water quality data from Swedish great lakes. *Geophysica*, *36*, 177–202.

Pope, R. M., & Fry, E. S. (1997). Absorption spectrum (380–700 nm) of pure water, 2, integrating cavity measurements. *Applied Optics*, *36*, 8710–8723.

Pulliainen, J., Kallio, K., Eloheimo, S., Koponen, H., Servomaa, T., Hannonen, S., Tauriainen, J., & Hallikainen, M. (2001). A semioperative approach to lake water quality retrieval from remote sensing data. *Science of Total Environment*, *268*, 79–93.

Simis, S. G. H., Peters, S. W. M., & Gons, H. J. (2005). Remote sensing of the cyanobacterial pigment phycocyanin in turbid inland water. *Limnology and Oceanography*, *50*(1), 237–245.

Tassan, S., & Ferrari, G. M. (2003). Variability of light absorption by aquatic particles in the near-infrared spectral region. *Applied Optical*, *42*(24), 4802–4810.

Thiemann, S., & Kaufman, H. (2000). Determination of chlorophyll contentand tropic state of lakes using field spectrometer and IRS – IC satellite data in the Mecklenburg Lake Distract, Germany. *Remote Sensing of Environment*, *73*, 227–235.

Tzortziou, M., Herman, J. R., Gallegos, C. L., Neale, P. J., Subramaniam, A., Harding, L. W., Jr., & Ahmad, Z. (2006). Bio-optics of the Chesapeake Bay from measurements and radiative transfer closure. *Estuarin, Coastal and Shelf Science*, *68*, 348–362.

Welschmeyer, N. A. (1994). Fluorometric analysis of chlorophyll a in the presence of chlorophyll b and pheopigments. *Limnology and Oceanography*, *39*, 1985–1992.

Zhang, Y. L., Zhang, B., Wang, X., Li, J. S., Feng, S., & Zhao, Q. H. (2007). A study of absorption characteristics of chromophoric dissolved organic matter and particles in Lake Taihu, China. *Hydrobiologia*, *592*, 105–120.

Zimba, P. V., & Gitelson, A. (2006). Remote estimation of chlorophyll concentration in hyper-eutrophic aquatic systems: Model tuning and accuracy optimization. *Aquaculture*, *256*, 272–286.